Basic Cumulus Dynamics

Clouds that occur when air becomes highly buoyant and accelerates upward in a localized region ($\sim$0.1–10 km horizontal extent) are referred to as *convective* or *cumuliform* clouds. Their vertical air motions are much stronger, and they condense and precipitate water more intensely. They all have the appearance of rapidly bubbling or "soaring" upward as they develop.

Cumuliform clouds exhibit a spectrum of forms, which include:

- *Fair weather cumulus*, which are $\sim$1 km in both horizontal and vertical scale (e.g., the cumulus humilis;
- *Cumulus congestus* (towering cumulus), which attain widths and depths of several kilometers as aggregates of discrete smaller buoyant bubbles within the cloud rise one after the other reaching successively greater heights ;
- *Individual cumulonimbus*, which can at times produce severe weather in the form of heavy rain, hail, lightning, thunder, strong outflow winds, and tornadoes. These clouds, occurring either alone or in lines, have widths on the order of tens of kilometers and typically extend vertically to near the tropopause, where their tops spread out and form the characteristic anvil, or "thunderhead";
- *Mesoscale convective systems*, which have cloud tops that extend over regions on the order of hundreds of kilometers in scale, produce large amounts of rain, contain stratiform precipitation that forms in connection with the cumulonimbus, and can develop mesoscale circulation patterns in addition to convective-scale air motions.

These different forms and degrees of convective cloud phenomena have several common dynamical characteristics. Fundamentally, they all arise from *buoyancy*; i.e., their air motions always originate in the form of vertical accelerations that occur when moist air becomes locally less dense than air in the surrounding larger scale environment. The buoyant accelerations lead to vertical air speeds $\sim$1–10 s of meters per second and to several important dynamical and physical phenomena that are associated with rapid local ascent and descent of air. The mass field in and around a convective cloud must adjust to the cloud's penetrative vertical motion, and a distinctive *buoyancy pressure-perturbation* field results to accommodate this adjustment. The rapidly moving air in convective clouds is turbulent, which leads to *entrainment* of surrounding environmental air. Entrainment in turn modifies the cloud dynamics and microphysics. Finally, the air motions in the cloud develop *rotation*, which can enhance entrainment and produce *dynamic pressure-perturbations* that can change the cloud's structure.

1 BUOYANCY

Since all convective clouds owe their existence to the fact that air becomes buoyant on a local scale (less than about 10 km), we begin by briefly recalling the nature of the buoyancy B, which appears as a contribution to vertical acceleration in the equation of motion. In the absence of friction, the vertical component of the momentum equation is:

$$\frac{\mathrm{D}w}{\mathrm{D}t} = -\frac{1}{\rho_o}\frac{\partial p^*}{\partial z} + B \qquad (1)$$

where w is the vertical velocity, ρ_o the reference-state density, and p^* the deviation of the pressure

7.2 THE PRESSURE-PERTURBATION FIELD ASSOCIATED WITH BUOYANCY

It can be anticipated intuitively that buoyancy cannot exist without a simultaneous disruption of the pressure field. If a parcel of air of finite width and depth is less dense than the air in a surrounding horizontally uniform and otherwise undisturbed atmosphere, then at the height of the base of the parcel, the pressure is lower in the parcel than in the environment. The horizontal gradient of pressure accelerates environmental air toward the base of the buoyant parcel. This inward acceleration, moreover, is consistent with the need to replace the buoyant air at the level that would otherwise be vacated by the upward moving parcel. A complete, internally consistent picture of mass, pressure, and momentum fields required to exist in association with a region of buoyant air is, of course, implied by the basic equations. We can obtain this picture by combining the horizontal and vertical equations of motion with the continuity equation. If friction and Coriolis forces are ignored, the equation of motion (2.47) can be written in Eulerian form as

$$\frac{\partial \mathbf{v}}{\partial t} = -\frac{1}{\rho_o}\nabla p^* + B\mathbf{k} - \mathbf{v}\cdot\nabla\mathbf{v} \tag{7.2}$$

If we take the three-dimensional divergence of this equation after first multiplying it by ρ_o, we obtain

$$\frac{\partial}{\partial t}(\nabla\cdot\rho_o\mathbf{v}) = -\nabla^2 p^* + \frac{\partial}{\partial z}(\rho_o B) - \nabla\cdot(\rho_o\mathbf{v}\cdot\nabla\mathbf{v}) \tag{7.3}$$

Making the anelastic approximation by assuming that mass continuity obeys (2.54), then the three-dimensional mass divergence in the anelastic system and hence the left-hand side of (7.3) is zero, and a diagnostic equation for the pressure perturbation is obtained:

$$\nabla^2 p^* = F_B + F_D \tag{7.4}$$

where

$$F_B \equiv \frac{\partial}{\partial z}(\rho_o B) \tag{7.5}$$

and

$$F_D \equiv -\nabla\cdot(\rho_o\mathbf{v}\cdot\nabla\mathbf{v}) \tag{7.6}$$

Thus, the Laplacian of the pressure-perturbation field in an anelastic fluid must be consistent with the vertical gradient of buoyancy F_B and the three-dimensional divergence of the advection field F_D. F_B is called the *buoyancy source* and F_D the *dynamic source*. The pressure perturbation may be thought of as the sum of two partial pressures p_B^* and p_D^* such that

$$p^* = p_B^* + p_D^* \tag{7.7}$$

$$\nabla^2 p_B^* = F_B \tag{7.8}$$

$$\nabla^2 p_D^* = F_D \tag{7.9}$$

In those relatively rare cases, $p^*{}_D$ dominates in certain parts of the cloud. In most convective cloud situations, however, the pressure perturbation $p^*{}_B$ determined, according to (7.5), by the vertical gradient of buoyancy dominates p^*.

To determine the nature of p_B^*, we note that (7.8) is analogous to Poisson's equation in electrostatics, where $-F_B$ plays the role of a charge density, p_B^* is like the electrostatic potential, and $-\nabla p_B^*$ is equivalent to the electric field. For simple spatial arrangements of buoyancy, we can thus use known mathematical solutions of Poisson's equations to find the vector field $-\rho_o{}^{-1}\nabla p_B^*$. We will call this field, which is analogous to an electric field produced by a particular spatial arrangement of charge density, the *buoyancy pressure-gradient acceleration (BPGA) field.*

This solution is illustrated qualitatively in Figure 1 for a uniformly buoyant parcel of finite dimensions. The plus

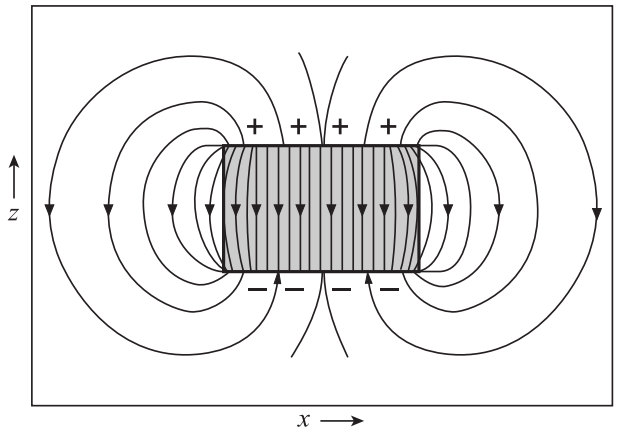

FIGURE 1 Vector field of buoyancy pressure-gradient force for a uniformly buoyant parcel of finite dimensions in the x–z plane. The plus and minus signs indicate the sign of the buoyancy forcing function $-\partial(\rho_o B)/\partial z$ along the top and bottom of the parcel.

and minus signs in the figure indicate the sign of $-F_B$ along the top and bottom of the parcel. Where $-F_B > 0$, the BPGA field (i.e., $-\rho_o^{-1}\nabla p_B^*$) diverges according to (7.8), and where $-F_B < 0$ the BPGA field converges. Everywhere except the top and bottom of the parcel, $F_B = 0$. The lines of the BPGA field are shown as streamlines, like lines of electric field for finite horizontal parallel plates of opposite charge density. Within the parcel, the lines of the BPGA field are downward. There is a divergence of the BPGA field at the top of the parcel and convergence at the bottom. Outside the parcel, lines of force are up above the parcel, downward in the regions to the sides of the parcel, and upward just below the parcel. These lines indicate the directions of forces acting to produce the compensating motions in the environment that are required to satisfy mass continuity when the buoyant parcel moves upward.

The downward lines of force shown inside the parcel in Figure 7.1 imply that the upward acceleration of buoyancy is counteracted to some degree by a downward BPGA. This counteraction must occur because some of the buoyancy of the parcel has to be used to move environmental air out of the way in order to preserve mass continuity while the parcel rises. The only way that downward BPGA could be absent would be to have the parcel's width shrink to zero—a nonsensical case, but nonetheless illustrative of the fact that *a given amount of buoyancy produces a larger upward acceleration the narrower the parcel*. In cumulus and cumulonimbus clouds, the distribution of B is such that BPGA is often the same order of magnitude as B. The BPGA can be especially important near the tops of growing clouds, where rising towers are actively pushing environmental air out of the way.

The maximum magnitude is achieved by the BPGA when it exactly balances B. If we let $B_o^* = 0$, then

$$B = \frac{1}{\rho_o}\frac{\partial p^*}{\partial z} = -\text{BPGA} \tag{7.10}$$

which is the case of hydrostatic balance (Section 2.2.4). In the strict mathematical sense, this case occurs at the limit where the horizontal dimension of a buoyant element as in Figure 7.1 becomes infinite in horizontal extent. This fact can be seen by multiplying (7.10) by ρ_o, taking $\partial/\partial z$ of both sides of the equation, and rearranging to obtain

$$\frac{\partial \rho_o B}{\partial z} = p_{zz}^* \tag{7.11}$$

Then (7.4), (7.5), and (7.11) imply that

$$\nabla_H^2 p^* = 0 \tag{7.12}$$

where ∇_H is the horizontal gradient operator. Thus, if the horizontal gradient of p^* is flat in at least one place, there is no horizontal variation of p^*. The counterpart of

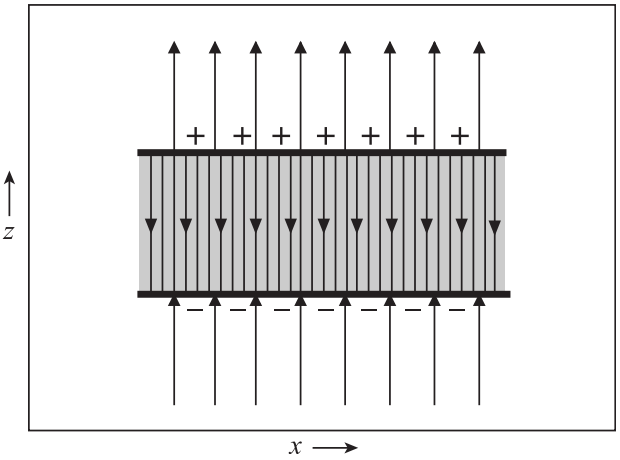

FIGURE 7.2 Vector field of buoyancy pressure-gradient force for a uniformly buoyant parcel of infinite horizontal dimensions. The plus and minus signs indicate the sign of the buoyancy forcing function $-\partial(\rho_o B)/\partial z$ along the top and bottom of the parcel.

Figure 7.1 for the hydrostatic case is shown in Figure 7.2, which shows the lines of force for a uniformly buoyant parcel of infinite horizontal extent.

3 ENTRAINMENT AND DETRAINMENT

3.1 General Considerations

Another important property common to all forms of convective clouds is that they are highly turbulent. Within convective clouds, buoyancy and gradients of velocity components are both strong. Hence, conversion from shear $\mathscr{C}$ and the buoyancy generation $\mathscr{B}$ in (2.86) are important sources of turbulent kinetic energy. The intensity of the turbulence in the cloud is much greater than in the surrounding environment.

The incorporation of environmental air into a cloud is called *entrainment*, while the ingestion of cloudy air into the laminar environment is referred to as *detrainment*. In the case of cumulus clouds, entrainment and detrainment are due not just to the turbulent mixing across boundaries but also to advection across the cloud boundaries required to satisfy mass continuity. In addition, air may be drawn into cumulus clouds as a result of internal cloud motions taking the form of organized overturning and rotation on the scale of the cloud itself.

In this section, we investigate the entrainment and detrainment processes that affect convective clouds. First,

we examine some early ideas about how to approximate the mixing at cloud boundaries. These traditional views regard the mixing as *continuous in time and homogeneous* in space. Then we will proceed to a more realistic view, which recognizes that the mixing is intermittent in time and inhomogeneous in space.

3.2 Early Views of Mixing with the Cloud's Environment

In the late 1940s, Henry Stommel, an oceanographer, suggested[1] that the turbulent exchange of mass between a cloud and its environment could be roughly approximated by considering a rising cloud element interacting with its environment as shown in Figure 7.3. At time t, the rising element is considered to have mass m. Between t and $t+\Delta t$, a mass of air $(\Delta\mathsf{m})_\varepsilon$ is entrained from the environment and a mass of air $(\Delta\mathsf{m})_\delta$ is detrained to the environment. Consider some quantity $\mathscr{A}$, which has units of energy, mass, or momentum per unit mass of air. The value of $\mathscr{A}$ in the rising cloud element is represented by $\mathscr{A}_c$ and in the environment by $\mathscr{A}_e$. It is assumed that we are dealing with horizontal averages for the in-cloud and out of cloud regions and that:

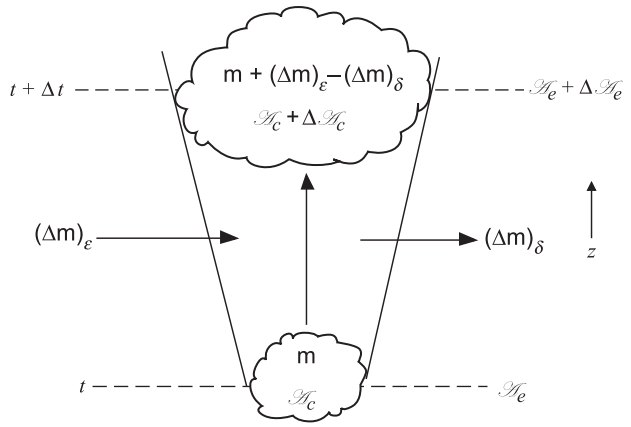

FIG 3 Idealization of a rising cloud element interacting with its environment.

- the entrained air is brought in from the sides (i.e., *laterally*),
- the entrained air is mixed *instantaneously* and *thoroughly* across the cloud element,
- and the process occurs *continuously* as the element rises.

These assumptions are the foundation of the concept of continuous, homogeneous entrainment. With these assumptions, the conservation of $\mathscr{A}$ in the cloud parcel can be written as

$$\begin{aligned}&\left[w+(\Delta\mathsf{m})_\varepsilon-(\Delta\mathsf{m})_\delta\right](\mathscr{A}_c+\Delta\mathscr{A}_c)\\&=\mathsf{m}\mathscr{A}_c+\mathscr{A}_e(\Delta\mathsf{m})_\varepsilon-\mathscr{A}_c(\Delta\mathsf{m})_\delta+\left(\frac{\Delta\mathscr{A}_c}{\Delta t}\right)_S\mathsf{m}\Delta t\end{aligned}\tag{7.13}$$

where $(\Delta\mathscr{A}_c/\Delta t)_S$ is the rate of change of $\mathscr{A}_c$ that would be present even if the parcel was not exchanging mass with the environment. Rearrangement of terms in (7.13) and taking the limit as $\Delta t\to 0$ leads to

$$\frac{\mathrm{D}\mathscr{A}_c}{\mathrm{D}t}=\left(\frac{\mathrm{D}\mathscr{A}_c}{\mathrm{D}t}\right)_S+\frac{1}{\mathsf{m}}\left(\frac{\mathrm{D}\mathsf{m}}{\mathrm{D}t}\right)_\varepsilon(\mathscr{A}_e-\mathscr{A}_c)\tag{7.14}$$

where the notation $\mathrm{D}/\mathrm{D}t$, as usual [see (2.2)], indicates a derivative following a parcel of fluid. The detrainment terms in (7.13) cancel and do not appear in (7.14) since *detrainment of mass in no way affects the mass averaged values of variables in the cloud*.[2] It is only entrainment that affects the in-cloud averages since it dilutes the parcel with environmental fluid.

As we will see in Sections 7.3.3–7.3.6, modern observations show that the entrainment and detrainment processes in cumulus clouds are *not* continuous, instantaneous, or thorough. A completely accurate representation of the process must ultimately take these facts into account. Nonetheless, the above simple view has considerable value in providing a simple and tractable first approximation to cumulus dynamics.

The role of entrainment in the First Law of Thermodynamics may be seen by applying (7.14) to the *moist static energy*

$$h\equiv c_pT+Lq_v+gz\tag{7.15}$$

In the absence of entrainment and diabatic processes other than release of latent heat in condensation or evaporation (ignoring ice-phase processes), the First Law is given by (2.12). If the pressure change following a parcel is to a first approximation hydrostatic, then taking D(7.15)$/\mathrm{D}t$, with substitution from (2.12) and (2.38), yields

$$\left(\frac{\mathrm{D}\mathscr{h}_c}{\mathrm{D}t}\right)_S = 0 \tag{7.16}$$

In this case, (7.14) becomes

$$\frac{\mathrm{D}\mathscr{h}_c}{\mathrm{D}t} = \frac{1}{\mathsf{m}}\left(\frac{\mathrm{D}\mathsf{m}}{\mathrm{D}t}\right)_\varepsilon (\mathscr{h}_e - \mathscr{h}_c) \tag{7.17}$$

when $\mathscr{h}$ is substituted for $\mathscr{I}$. Using the definition (7.15), we may rewrite (7.17) as

$$\frac{\mathrm{D}T_c}{\mathrm{D}t} = \underset{(i)}{-\frac{g}{c_p}w_c} \underset{(ii)}{-\frac{L}{c_p}\frac{\mathrm{D}q_v}{\mathrm{D}t}} + \underset{(iii)}{\frac{1}{\mathsf{m}}\left(\frac{\mathrm{D}\mathsf{m}}{\mathrm{D}t}\right)_\varepsilon \left[(T_e - T_c) + \frac{L}{c_p}(q_{ve} - q_{vc})\right]} \tag{7.18}$$

where the terms on the right are recognized to be (i) the dry adiabatic cooling, (ii) the latent heating, and (iii) the effects of mixing.

Equations of the form (7.14) may also be written with $\mathscr{I}$ replaced by the vertical velocity or the water-continuity variables in a cumulus cloud. In the case of vertical velocity, the source term in (7.14) (i.e., the change in w that would occur whether or not entrainment takes place) becomes $(\mathrm{D}w_c/\mathrm{D}t)_S$, which is given by the right-hand side of (7.1). Thus, (7.14) becomes

$$\frac{\mathrm{D}w_c}{\mathrm{D}t} = -\frac{1}{\rho_e}\frac{\partial p^*}{\partial z} + B - \frac{1}{\mathsf{m}}\left(\frac{\mathrm{D}\mathsf{m}}{\mathrm{D}t}\right)_\varepsilon w_c \tag{7.19}$$

which is equivalent to adding the entrainment term to (7.1). The reference-state density has been taken to be that of the environment, whose conditions can be obtained from radiosonde data. The vertical velocity in the environment does not appear in the entrainment term because it is assumed to be small compared to the vertical velocity in the cloud.

When $\mathscr{I}$ is replaced by the water substance mixing ratios, the change in the mixing ratio that would occur in the absence of entrainment $(\mathrm{D}q_{ic}/\mathrm{D}t)_S$ is given by the sources and sinks represented by S_i on the right-hand side of the water-continuity equations (2.21). The water-continuity equations then take the form

$$\frac{\mathrm{D}q_{vc}}{\mathrm{D}t} = -C + \frac{1}{\mathsf{m}}\left(\frac{\mathrm{D}\mathsf{m}}{\mathrm{D}t}\right)_\varepsilon (q_{ve} - q_{vc}) \tag{7.20}$$

and

$$\frac{\mathrm{D}q_{ic}}{\mathrm{D}t} = S_i + \frac{1}{\mathsf{m}}\left(\frac{\mathrm{D}\mathsf{m}}{\mathrm{D}t}\right)_\varepsilon (q_{ie} - q_{ic}), i = 1, \ldots, k \tag{7.21}$$

where C, representing the net condensation (or evaporation) rate, is the sink (or source) term for the water-vapor mixing ratio, k is the number of subdivisions of the hydrometeor content, and the source and sink terms for these mixing ratios depend upon the type of water-continuity model assumed and are therefore left in symbolic form as S_i.

Equations (7.18)–(7.21) would constitute a way to calculate the properties T_c, w_c, q_{vc}, and q_{ic} of a rising parcel in a cumulus cloud, if ways of determining the pressure perturbation p^* and the entrainment rate $\mathsf{m}^{-1}(\mathrm{D}\mathsf{m}/\mathrm{D}t)_\varepsilon$ were available. This set of equations is the basis of the *one-dimensional Lagrangian cumulus model*. Often, this model is expressed with z rather than t as the coordinate. The vertical velocity $w = \mathrm{D}z/\mathrm{D}t$ is used as the basis for the coordinate transformation. By substituting $w\mathrm{D}/\mathrm{D}z$ for $\mathrm{D}/\mathrm{D}t$ in (7.18)–(7.21) and dividing all the equations by w (assumed to be finite and positive for a rising mass of fluid), we obtain

$$\frac{\mathrm{D}T_c}{\mathrm{D}z} = -\frac{g}{c_p} - \frac{L}{c_p}\frac{\mathrm{D}q_{vc}}{\mathrm{D}z} + \Lambda\left[(T_e - T_c) + \frac{L}{c_p}(q_{ve} - q_{vc})\right] \tag{7.22}$$

$$\frac{\mathrm{D}}{\mathrm{D}z}\left(\frac{1}{2}w_c^2\right) = -\frac{1}{\rho_e}\frac{\partial p^*}{\partial z} + B - \Lambda w_c^2 \tag{7.23}$$

$$\frac{\mathrm{D}q_{vc}}{\mathrm{D}z} = -\frac{C}{w_c} + \Lambda(q_{ve} - q_{vc}) \tag{7.24}$$

and

$$\frac{\mathrm{D}q_{ic}}{\mathrm{D}z} = \frac{S_i}{w_c} + \Lambda(q_{ie} - q_{ic}), i = 1, \ldots, k \tag{7.25}$$

where

$$\Lambda \equiv \frac{1}{\mathsf{m}}\left(\frac{\mathrm{D}\mathsf{m}}{\mathrm{D}z}\right)_\varepsilon \tag{7.26}$$

It should be noted that the values of T_c, w_c, q_{vc}, and q_{ic}, obtained as solutions of (7.22)–(7.25), are values of these variables at various points along the path of a cloud element that is either rising or sinking. These solutions are not instantaneous in-cloud profiles except in the special case of a steady state cloud in which similar parcels continually follow each other upward.

Equation (7.22) can be thought of in terms of a thermodynamic diagram. The left-hand side gives the temperature change of the parcel with height. The first two terms on the right describe the temperature change with height of the parcel in the presence of condensation but in the absence of entrainment. The negative of this temperature change with height is the *moist adiabatic lapse rate*. If entrainment is active, the lapse rate of a parcel $(-\mathrm{D}T_c/\mathrm{D}z)$ lies somewhere between the moist adiabatic and environmental lapse rate as a result of mixing environmental air of different temperature and humidity into the parcel. If the entrainment effect is strong, the parcel's temperature differs only slightly from the environmental temperature. Thus, this simple view seems to explain qualitatively the observations that Stommel was concerned about (see earlier footnote).

To close the one-dimensional Lagrangian cumulus model, some way has to be found to express the entrainment

Λ and the pressure perturbation p^*. The traditional approach is to invoke some form of mass continuity, while considering the cumulus cloud to be analogous to certain laboratory phenomena. For this purpose, three types of laboratory phenomena are considered: the *jet*, the *thermal*, and the *starting plume*.

In the jet model, the updraft is considered to behave, to a first approximation, like a steady state, mechanically driven jet (Figure 7.4). In such a jet, environmental fluid is entrained and, since the environment is relatively laminar, there is no detrainment from the jet (i.e., the environment does not entrain air from the jet). Consider an arbitrary parcel of mass m between heights z and $z+\Delta z$ in the idealized steady state jet depicted in Figure 7.5. In time Δt, the original mass m is replaced by an equal mass. Therefore,

$$\mathsf{m} = \mu_f \Delta t \tag{7.27}$$

where μ_f is the vertical mass *flux* (in kg s^{-1}) in the jet at height z. Also in time Δt, the original parcel entrains mass

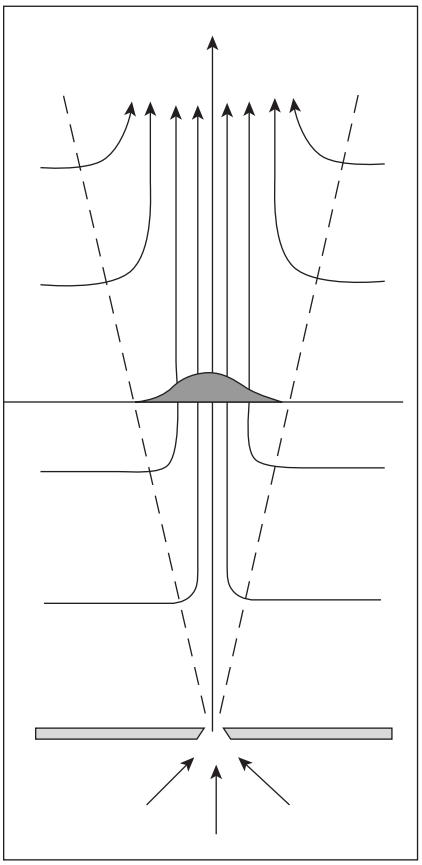

FIGURE 7.4 Streamlines of the flow associated with a mechanically driven fluid jet. The cross sectional area of the jet expands downstream from its source as fluid is entrained from the environment.

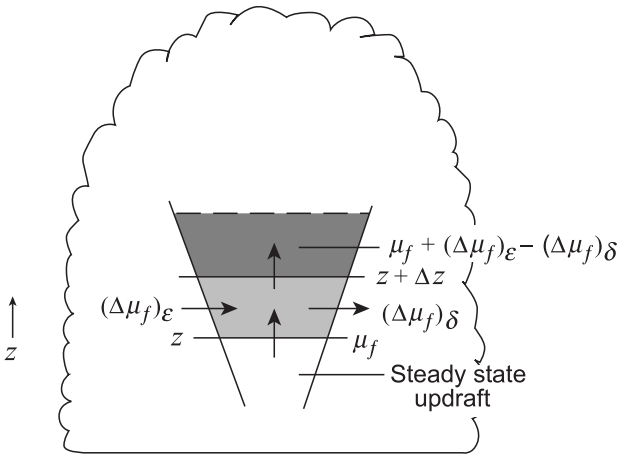

FIGURE 7.5 Idealization of a steady state updraft jet inside a cumulus cloud.

$$(\Delta\mathsf{m})_\varepsilon = (\Delta\mu_f)_\varepsilon \Delta t \tag{7.28}$$

It follows from (7.27) and (7.28) that, for a steady state jet

$$\frac{1}{\mathsf{m}}(\Delta\mathsf{m})_\varepsilon = \frac{1}{\mu_f}(\Delta\mu_f)_\varepsilon \tag{7.29}$$

The entrainment rate Λ defined by (7.26) is then obtained for the steady state jet by dividing (7.29) by Δz and taking the limit as $\Delta z \to 0$; the result is:

$$\Lambda = \frac{1}{\mu_f}\left(\frac{d\mu_f}{dz}\right)_\varepsilon \tag{7.30}$$

where we have made use of the fact that in the special case of a steady state jet the vertical derivative following the parcel D/Dz and the vertical derivative with respect to height at an instant of time within the steady state jet d/dz are equivalent.

The mean flow in laboratory jets is approximately steady state, incompressible, and circularly symmetric. Under these conditions the mean-variable form of the Boussinesq mass continuity equation (2.55) applies. In cylindrical coordinates centered on the jet, which is assumed to be circularly symmetric about the central axis, this equation becomes

$$\frac{1}{r}\frac{\partial(r\overline{\mathsf{u}})}{\partial r} + \frac{\partial\overline{w}}{\partial z} = 0 \tag{7.31}$$

where r is the radial coordinate and u is the radial velocity. Bars indicate time averages. Laboratory experiments with this type of jet show that

$$\overline{w} = W(z)e^{-(r/\hat{R})^2} \tag{7.32}$$

where $\hat{R}$ is a constant.[3] Other dynamical variables have similar radial profiles. For mathematical simplicity, this Gaussian profile is often replaced by a "top hat" profile:

$$\overline{w} = \begin{cases} w_c(z), & 0 < r < b \\ w_e(z), & r > b \end{cases} \tag{7.33}$$

Substituting this profile into (7.31) and integrating over radius from 0 to b, we obtain

$$\frac{\mathrm{d}}{\mathrm{d}z}\left(w_c b^2\right) = -2b\overline{u}(b) \tag{7.34}$$

Thus, an increase in mass flux with height is matched by horizontal inflow.

In early experiments with laboratory jets, it was hypothesized[4] and verified experimentally that the horizontal inflow at a given altitude was proportional to the rate of upward motion at that level, that is:

$$-\overline{\mathrm{u}}|_{r=\hat{R}} = \alpha_\varepsilon W \tag{7.35}$$

where α_ε stands for a constant determined from laboratory experiments. If for the top hat approximation we associate $\hat{R}$ with b, we infer from (7.34) and (7.35) that

$$\frac{\mathrm{d}}{\mathrm{d}z}\left(w_c b^2\right) = 2\alpha_\varepsilon b w_c \tag{7.36}$$

Since $w_c b^2$ is proportional to the vertical mass flux in the jet (μ_f), (7.36) can be rewritten as

$$\frac{1}{\mu_f}\frac{\mathrm{d}\mu_f}{\mathrm{d}z} = \frac{2\alpha_\varepsilon}{b} \tag{7.37}$$

Recalling (7.30), and the fact that the laboratory jets do not detrain, we see that (7.37) gives us an expression for the entrainment rate.

$$\Lambda = \frac{1}{\mu_f}\left(\frac{\mathrm{d}\mu_f}{\mathrm{d}z}\right)_\varepsilon = \frac{2\alpha_\varepsilon}{b} \tag{7.38}$$

The shape of the jet implied by (7.36) is given by

$$\frac{\mathrm{d}b}{\mathrm{d}z} = -\frac{1}{2}b\frac{\mathrm{d}\ln w_c}{\mathrm{d}z} + \alpha_\varepsilon \tag{7.39}$$

Laboratory data show that α_ε has a value of about 0.1.

The laboratory jets to which (7.38) applies are incompressible. The analogy between the cumulus clouds and the laboratory jet is based on the similarity of the incompressible and anelastic continuity equations. The incompressible equation is identical to the Boussinesq equation (2.55). The anelastic continuity equation (2.54) differs only in the inclusion of the density-weighting factor ρ_o, which we set equal here to the environmental density ρ_e. For the steady state cylindrical geometry of the jet, the anelastic continuity equation is then

$$\frac{1}{r}\frac{\partial(\rho_e r\overline{\mathrm{u}})}{\partial r} + \frac{\partial(\rho_e \overline{w})}{\partial z} = 0 \tag{7.40}$$

which is similar to (7.31) except for the density factor. By analogy to the incompressible case, the equivalent to (7.39) is found to be

$$\frac{\mathrm{D}b}{\mathrm{D}z} = -\frac{1}{2}b\frac{\mathrm{D}}{\mathrm{D}z}\ln(\rho_e w_c) + \alpha_\varepsilon \tag{7.41}$$

where we have replaced the notation $\mathrm{d}/\mathrm{d}z$ with $\mathrm{D}/\mathrm{D}z$ to emphasize that this equation can be solved simultaneously with (7.22)–(7.25) in the case of the steady state jet.

To complete the jet-analogy version of the one-dimensional Lagrangian cumulus equations, it is assumed that the pressure perturbation is zero, and a laboratory derived empirical value of $\alpha_\varepsilon = 0.1$ is usually used in (7.38) and (7.41). The vertical equation of motion (7.23) then becomes

$$w_c\frac{\mathrm{D}w_c}{\mathrm{D}z} = B - \frac{0.2}{b}w_c^2 \tag{7.42}$$

It is evident from Section 7.2 that the assumption of zero pressure perturbation (or that its vertical gradient is zero) violates mass continuity. The assumption in this case can be partially justified since once a steady state jet is established, a rising parcel inside the jet does not have to do much work to push the fluid ahead of the parcel out of the way since the parcel lying in its path is already in motion. Hence, the vertical pressure-gradient acceleration is not large. The steady state jet analog model of cumulus convection is then constituted by the equations (7.22), (7.24), (7.25), (7.38), (7.41), and (7.42) in the variables T_c, w_c, q_{vc}, q_{ic}, Λ, and b. The source and sink terms C and S_i are expressed in terms of these variables to close the set of equations.

Various objections were raised to the jet analogy as a model of cumulus convection. This model in particular does not appear to account for the non-steady aspects of many convective clouds. These objections led to the *bubble model*,[5] in which a cumulus cloud is envisioned as a series of rising bubbles of buoyant air. As each bubble rises, environmental air is pushed around the bubble and mixes into a turbulent wake behind the bubble. As the environmental air moves around the bubble, it continually erodes the surface layer of the bubble until the entire bubble disappears. A new bubble may rise through the wake of a previous bubble. Since the wake contains more water vapor than the surrounding environment, the new bubble is exposed to successively less erosion and can therefore attain a greater altitude than its predecessor. A cumulus cloud is envisioned as consisting of new bubbles rising through the wakes of old

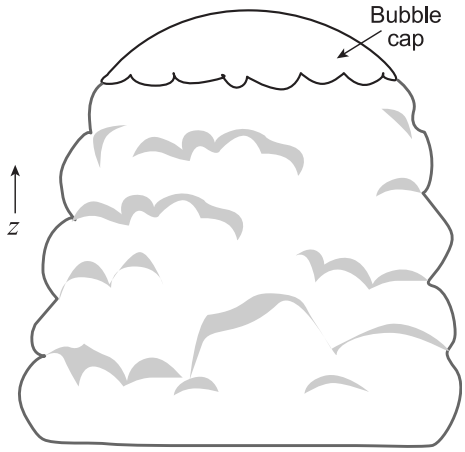

FIG 6 Bubble model of convection.

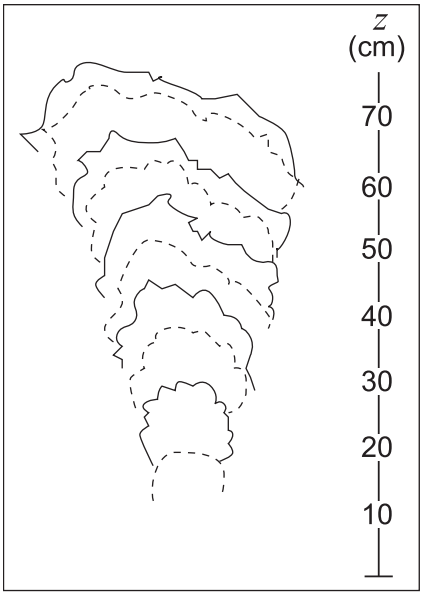

FIGURE 7.7 Successive outlines of laboratory thermals traced from photographs. The thermals, produced by dropping elements of salt solution into water, were negatively buoyant. The picture is inverted to indicate the analogous ascent of a positively buoyant element.

bubbles. The top of the cloud consists of the upper cap of the most highly ascending bubble in the cloud (Figure 7.6). The bubble model has qualitative appeal in that it seems to retain the character of what many cumulus clouds look like as they grow.

A quantitative formulation of the bubble model[6] assumes that the rising bubbles are spherical and preserve their shape while diminishing in size. The vertical momentum equation (7.23) is then written as

$$w_c \frac{\mathrm{D}w_c}{\mathrm{D}z} = -D_R + B \tag{7.43}$$

where $-D_R$ is a parameterization of the vertical pressure-gradient acceleration term.[7] According to this model, $\Lambda = 0$. That is, the buoyant elements do not entrain. They only detrain as they are eroded. The erosion rate may be related, according to a prescribed scheme, to the thermodynamic properties of the environment. The environmental air is, however, not mixed into the remaining non-eroded core, and entrainment terms do not appear in any equations. Thus, buoyancy is counteracted in the vertical motion equation (7.43) entirely by the pressure-gradient acceleration, not by diluting the buoyancy by entrainment of environmental air. This characteristic of the bubble model appears to be in contradiction to the observations of diluted air in cumulus—such as those discussed by Stommel. For this reason, the bubble model was disregarded for many years.

When elements of salt solution were released into water, it was found that these (negatively) buoyant ele-ments were not eroded, but rather expanded (Figure 7.7). Thus, it was discovered that bubbles are not simply eroded; they also entrain. These entraining buoyant bubbles are referred to as *thermals*. The laboratory experiments showed that erosion (detrainment) occurred only in a stratified stable environment. In the atmosphere, evaporative cooling around the edges of rising cloud elements can contribute to the tendency of mixtures to be left behind, enhancing bubble model tendencies.

Laboratory thermals in a neutral environment were observed to expand along a similar cone for which the radius of a thermal was given by

$$b = \alpha_\varepsilon z \tag{7.44}$$

where z is the height of the center of the thermal and $\alpha_\varepsilon = 0.2$. Since the thermal does not detrain, its entrainment rate is

$$\frac{1}{\mathrm{m}}\left(\frac{\mathrm{Dm}}{\mathrm{D}t}\right)_{\varepsilon}=\frac{1}{(4/3)\pi b^3}\frac{\mathrm{D}}{\mathrm{D}t}\left[(4/3)\pi b^3\right] \tag{7.45}$$

Substituting from (7.44) and dividing by w_c, we obtain

$$\Lambda=\frac{1}{\mathrm{m}}\left(\frac{\mathrm{Dm}}{\mathrm{D}z}\right)_{\varepsilon}=\frac{3\alpha_{\varepsilon}}{b} \tag{7.46}$$

where $\alpha_{\varepsilon}=0.2$. Comparing (7.38) and (7.46), we note that the entrainment rates for jets and thermals are both inversely proportional to the radius of the region of rising fluid, but the entrainment rate for the thermal is $3\times$ larger than for the jet.

Making use of (7.46) and the empirical value of $\alpha_{\varepsilon}=0.2$, we may write the vertical momentum equation (7.23) in the case of the thermal as

$$w_c\frac{\mathrm{D}w_c}{\mathrm{D}z}=-D_R+B-\frac{0.6}{b}w_c^2 \tag{7.47}$$

This relation has similarities to the momentum equations for both the jet (7.42) and the bubble (7.43). Like the jet equation, it has an entrainment term. The rate of entrainment, however, is now proportional to $0.6/b$, which is triple the rate of dilution in the jet. Moreover, the buoyancy B is much weaker since the temperature and mixing ratio equations also contain entrainment terms diluting the in-cloud thermodynamic properties—at a rate of $0.6/b$. In addition, a parameterized pressure-gradient acceleration is again included, since, like the bubble, the thermal must push the environmental air out of the way. Thus, the thermal has both high entrainment and pressure drag slowing it down, and low buoyancy.

The laboratory experiments such as those illustrated in Figure 7.7 reveal not only that the thermal entrains, but they also indicate the mechanism of entrainment in these phenomena. It was found that the internal circulation in laboratory thermals is similar to that of a Hill's vortex (cf. Figures 7.8 and 7.9a). Hill vortex theory[9] has been used[10] to derive an analytic expression for the observed internal circulation in a rising cumulus-cloud element. According to this model, the upper portion of the cloud element consists of a Hill's vortex with a turbulent wake located somewhere below the center of the cloud element (Figure 7.9b). The upward circulation in the center of the element described by the Hill's vortex is the mechanism of entrainment. This upward influx into the element is assumed to come from the wake and thus to be composed of an arbitrary mixture of environmental and undiluted cloud air.

A relationship between jets and thermals was discovered as the laboratory experiments continued into the early 1960s. Specifically, it was found that as a laboratory

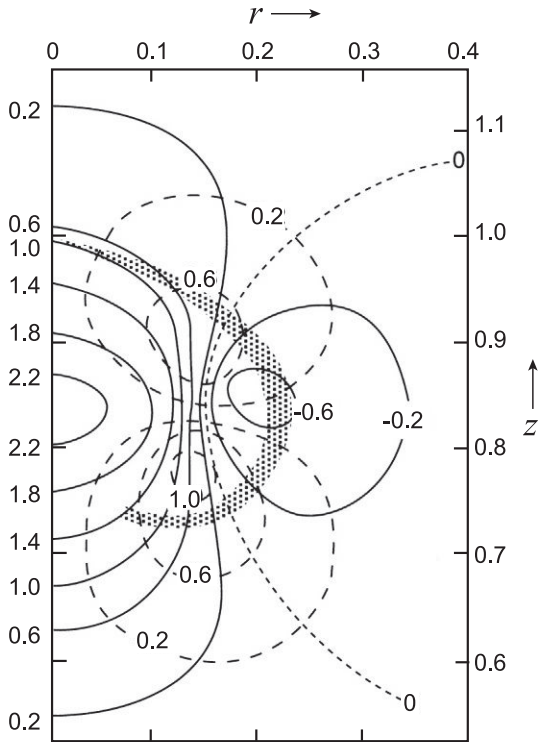

FIG 8 The distribution of velocity in a laboratory thermal. The outline of the buoyant fluid is shaded. The values of the vertical velocities (solid lines) and radial velocities (dashed lines) are expressed as multiples of the vertical velocity of the thermal cap.

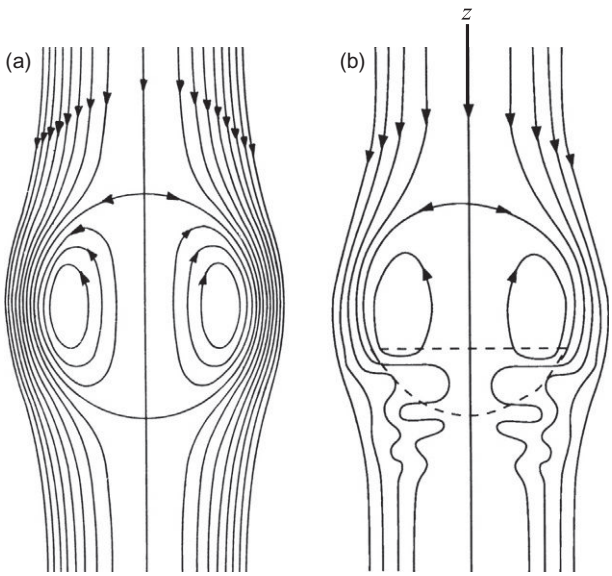

FIG 9 (a) Theoretical "Hill's vortex." Stream function lines both inside and outside the vortex are shown. (b) Idealization of the internal circulation in a rising cumulus-cloud element. The upper portion consists of Hill's vortex. The lower portion, located below the center of the cloud element, is a turbulent wake.

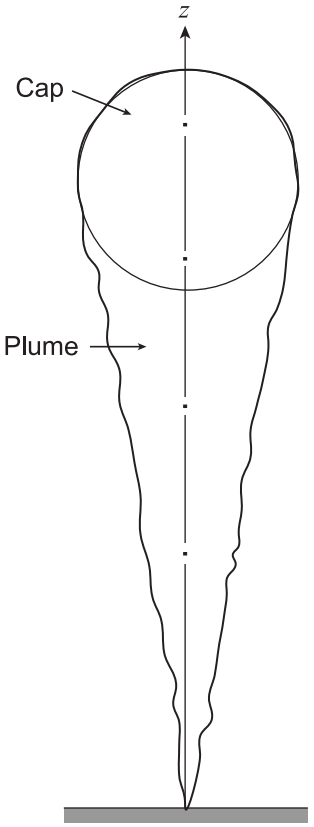

FIG 10 The "starting plume," which occurs as a turbulent jet begins.

jet becomes established, it is capped by a thermal (Figure 7.10). This entity is called the *starting plume*. It is modeled by assuming that the cap behaves like a thermal, except that the fluid just below the cap is characterized by the solution of the steady state jet equations. That is, fluid drawn up into the cap comes from the jet and is thus already a mixture of cloud and environmental air. The cap should therefore be diluted more slowly than an isolated thermal of the same size under similar environmental conditions. The vertical velocity in the jet, which has the Gaussian profile (7.32), almost exactly matches the analytic expression for the vertical velocity profile in the spherical vortex (Figure 7.11). This coincidence allows one to derive a set of equations for the plume cap taking into account the influx of air from the Gaussian plume at the base of the cap.[12] The entrainment rate predicted by these equations is inversely proportional to the cap radius. Laboratory experiments verified this relation and showed the proportionality constant was 0.2, that is:

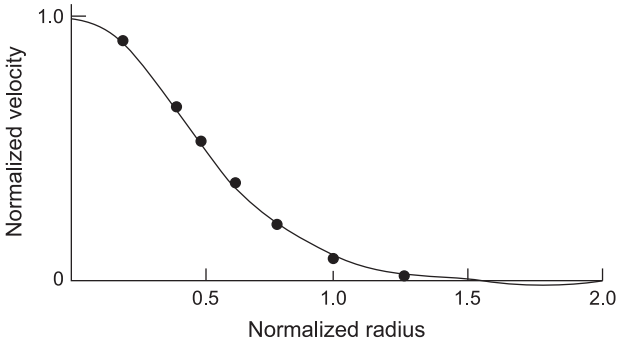

FIG 11 Matching of the vertical velocity in the lower jet (dots) and the upper spherical vortex (solid line) of a starting plume.

$$\Lambda = \frac{1}{m}\left(\frac{Dm}{Dz}\right)_{\varepsilon} = \frac{0.2}{b} \tag{7.48}$$

for the starting plume cap. The equation for the vertical velocity of the cap can then be written as

$$w_c \frac{Dw_c}{Dz} = -D_R + B - \frac{0.2}{b} w_c^2 \tag{7.49}$$

which has the form of (7.47), the equation for the thermal, but with an entrainment rate equal to that of the steady state jet [recall (7.38)].

During the mid- to late 1960s, the one-dimensional Lagrangian model was tested extensively in the field as a way to predict the maximum height reached by a convective cloud. In these tests, the cloud element radius b was treated as an observed quantity provided by visual observation from research aircraft flying near the clouds. For simplicity, b was assumed to be a constant for a particular cloud. The thermodynamic structure of the environment was provided by radiosonde data taken in the vicinity of the clouds. It was found that the most accurate cloud-top heights were calculated for an entrainment rate of approximately $0.2/b$, which corresponds to both the jet and the starting plume analogy.[13] Cloud-top height, however, is not an especially good test of the cloud dynamics since it is basically the stability of the environment that controls cloud height rather than any assumed model properties. Extensive experimentation has shown that one-dimensional Lagrangian models are incapable of simultaneously predicting cloud-top height and liquid water content.